Renormalization-group calculation for electrons in a half-filled Landau level

S. T. Chui
Bartol Research Institute, University of Delaware, Newark, Delaware 19716
(Received 19 March 1993)

The major obstacle for analytic calculations for electrons in the lowest Landau level arises from the degeneracy of the single-particle eigenstates. When the electron-electron interaction is included, the diagonal energy of different basis states is no longer the same and degenerate perturbation theory can be carried out. The near degeneracy of the single-particle states is manifested as an infrared-divergent perturbation series which is similar to that of a collection of one-dimensional interacting spinless chains. Thus a renormalization-group scheme can be developed. The range of the interparticle potential affects the change in diagonal energy for particle-hole fluctuations. For the Coulomb potential we find that the coupling constants remain unchanged over many length scales. The system remains gapless, consistent with recent transport and surface-acoustic-wave measurements.

I. INTRODUCTION

The discovery of the integer and fractional quantized Hall effect (FQHE) has generated much excitement recently. The FQHE is believed to come at odd-denominator filling factors so that the ground state does not possess long-range positional order and a gap exists in its excitation spectrum. As of yet the study of the physics of the ground state at other filling factors such as those with even denominators or at low densities is still in its infancy.

The first violation of the odd-denominator rule occurs at $\nu=\frac{5}{2}$ and is interpreted as being due to a spin effect.[1] Violations of the odd-denominator rule because of different physics at half-filling for narrow channels were predicted by Chui.[2,3] This phenomenon was subsequently observed by Timp *et al.*[4] For two-dimensional (2D) samples at even-denominator filling factors such as one-half, Jiang *et al.*[5] found a dip in the longitudinal resistivity but no Hall plateau, a finding very different from that of the conventional FQHE. This was interpreted[6] in terms of a quasisolid wave function with algebraic long-range positional order previously considered by Chui, Ma, and Hakim.[7] This coherent state of intermediate long-range order which we called a *marginal solid* presents interesting features in its excitation spectrum. The phonon excitations, which were the Goldstone modes when the long-range order was completely broken, are no longer gapless because the long-range order is only algebraic. Gapless excitations corresponding to the Goldstone mode that consists of density fluctuations can still be constructed from this wave function, however. The possibility of a marginal solid phase at half-filling is also suggested by variational[7] and finite-size scaling[8] calculations.

Other possible ground states at half-filling have also been proposed. Kuramoto and Gerhardts[9] have studied a charge-density wave (CDW) state with long-range order at half-filling with mean-field theory and found that the square lattice is more stable than the triangular (hexagonal) lattice. Fano, Ortolani, and Tosatti[10] have considered the triangular lattice with long-range order and its coexistence with hexagonal lattices and the question of particle-hole symmetry. Recently Halperin, Lee, and Reed [11] conjectured that the half-filled state is a fluid also with gapless excitations. They found logarithmic corrections that suggest an infinite mass and argue that many features of the fluidlike behavior remain. We do not know at the moment whether this description implies the same result as ours. After all, an infinite mass suggests a very high density of states and a concomitant Fermi surface instability, which may lead back to a solid. For example, for an ordinary Fermi fluid with a Coulomb interaction, a large mass implies a small Bohr radius and a large r_s, implying a Wigner instability in a solid. To better understand the nature of the ground state, we have carried out a systematic analytic renormalization-group (RG) calculation in this paper.

The major obstacle for analytic calculations for electrons in the lowest Landau level arises from the degeneracy of the single-particle eigenstates. When the electron-electron interaction is included, the diagonal energy of different basis states is no longer the same, however. Thus degenerate perturbation theory can be carried out by starting from the state with the lowest diagonal energy. This paper reports the result of such a calculation. The state with the lowest diagonal energy consists of a periodic array of clusters as is illustrated in Fig. 1. This is similar to a collection of Fermi surfaces as in a collection of 1D chains. For particle-hole excitations with

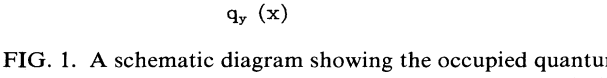

FIG. 1. A schematic diagram showing the occupied quantum numbers ("sites" or y momentum in the Landau gauge) (solid line) and the unoccupied sites (dotted lines) for the state with the lowest diagonal energy.

0163-1829/93/48(23)/17343(7)/$06.00

momentum transfer q, the change in diagonal energy is proportional to $q \ln q$ for the Coulomb potential and to q for short-range potentials. The near degeneracy of the single-particle states is manifested as an infrared divergent perturbation series which is similar to that of a collection of 1D interacting spinless chains. Thus a RG scheme can be developed. We find that the coupling constants remain unchanged over many length scales. Thus the system behaves as if it is at "criticality" for all practical purposes.

Recent surface-acoustic-wave measurements[12] and transport measurements near half-filling[13] suggest the absence of a gap but do not settle the issue of marginal solid versus fluidlike behavior.

II. RG CALCULATION

A. "Unperturbed ground state" and single-particle excitation energies

We first discuss the configuration with the lowest diagonal energy. One can use either the angular momentum gauge or the Landau gauge in describing the single-particle eigenstates. In this paper we use the Landau gauge under rectangular boundary conditions with aspect ratio $a=L_x/L_y=2/\sqrt{3}$; commensurate with the triangular Wigner lattice, the results for the angular momentum gauge will be similar. Many particle states can be constructed from Slater determinants of the product of the single-particle states. These many-particle states possess different Coulomb energy. We pick the configuration of the electrons that minimizes the diagonal part of the Hamiltonian and investigate systematically the particle-hole excitations away from it.

The Landau orbital is characterized by its y momentum $2\pi j/L_y$ and is given by (distances are expressed in units of the cyclotron radius in this paper)

$$\phi_j(\mathbf{r})=\exp[ix_j y-(x-x_j)^2/2]/(\pi^{1/2}L_y)^{1/2}\ , \qquad x_j=bj,\quad b=2\pi/L_y\ . \tag{1}$$

The Hamiltonian in second quantized form can be written, except for trivial constants, as

$$H=\sum_{[j]} A(j_1,j_2,j_3,j_4)C^\dagger_{j_1}C^\dagger_{j_2}C_{j_3}C_{j_4}\ . \tag{2}$$

The As are integrals of the Coulomb potential and the Landau orbitals ϕ_js. It is given by

$$A(j_{23},j_{13})=\sum_{j_x=-\infty}^{\infty} U[(j_x^2/a+j_{23}^2 a)^{1/2}] \times\exp[-(j_x^2/a+j_{23}^2 a)\pi/N_s] \times\cos(2\pi j_x j_{13}/N_s)\sqrt{\pi/2N_s}\ . \tag{3}$$

$U(q)=e^2/2\pi\epsilon lq$ is the Fourier transform of the interparticle potential. When the momentum transfer j_{23} is small, $A\approx 1/j_{23}$. This divergence is due to the well-known long-range nature of the Coulomb potential. In this paper we shall also discuss the effect of a short-range interaction. For a δ-function interaction its Fourier transform $U(q)=U_0$ is a constant. In that case

$$A'(u,y)=U_0\int_{-\infty}^{\infty} dx\ \exp[-(x^2/a+y^2 a)\pi] \times\cos(2\pi xu)\sqrt{\pi/2N_s} =U_0\exp[-(u^2+y^2)a\pi]\sqrt{a\pi^2/2N_s} \tag{4}$$

is symmetric with respect to its two arguments. There is a similarity between (2) and the Hubbard model. To bring out this similarity and to gain more insight, we decompose the Hamiltonian as a sum of a diagonal H_d and an off-diagonal H_o term as

$$H=H_d+H_o\ ,$$

$$H_d=\sum_{k,j} V(k)n_j n_{j+k}\ , \tag{5}$$

$$H_o=\sum_{l=1}\sum_{k=1} t_l(k)\sum_i C^\dagger_{i-l}C_i C_{i+k}C^\dagger_{i+k+l}+\text{c.c.} \tag{6}$$

The t's are the hopping integrals.

The configuration that minimizes the diagonal energy depends on the form of $V(k)$. At large k, $V(k)$ decreases as k is increased because of the repulsive nature of the Coulomb potential. However, it also possesses an attractive part as a result the exchange so that as k approaches the origin $V(k)$ attains a maximum and then decreases.[14] More precisely,

$$V(k)=2[A(j_{23}=0,j_{13}=k)-A(j_{23}=k,j_{13}=0)]\ , \tag{7}$$

where $j_{ab}=j_a-j_b$; the first (second) is the direct (exchange) contribution. At small distances k, these two terms are comparable in magnitude; the net value of V is reduced. As k increases, the exchange contribution dies off exponentially fast and only the first term remains.[14] The distance l_t at which V turns from repulsive to attractive is independent of the sample size N_s. Because of this attractive part of V, the particles have a tendency to form clusters with N_c contiguous occupied sites separated from each other by N_c empty sites. $N_c\approx[\sqrt{\nu N_s}]$, ν is the filling factor, N_s is the total number of electrons. The square bracket means the integer closest to N_c. This is illustrated in Fig. 1. For systems with less than 16 electrons, we have enumerated all possible states and verified that this is indeed the lowest energy configuration. As we discuss in Appendix A, the ground state from small cluster exact diagonalization is also dominated by this kind of cluster configuration. Our RG calculation does not depend on the precise value of the intercluster separation. It only depends on the fact that the array of clusters is a minimum of the diagonal part of the Hamiltonian.

We next investigate the fluctuations from the cluster configuration due to the off-diagonal part of the Hamiltonian H_o. Each of the clusters can be regarded as a 1D Fermi sea with a Fermi momentum $k_F=\sqrt{\pi\nu/\sqrt{3}}$. The total system consists of an array of N_c such clusters labeled by cluster indices l. The diagonal part H_d provides for a self-energy which acts as an effective kinetic energy for the particle-hole excitations away from the cluster configuration. These self-energy corrections render the particle-hole excitations nondegenerate; thereby facilitating the perturbation calculation. This is the essential

idea behind conventional degenerate perturbation theory. We now describe the change of this diagonal energy.

The energy for particle-hole excitations is the sum of the energies for particle excitation and hole excitation. Because of particle-hole symmetry, the particle excitation energy is the same as the hole excitation energy. When a particle is taken from site $k-1$ to k the energy change is

$$\Delta E(k)=\sum_{n=0}^{n=N_c-1} V(nN_i+N_c+k-1)-V(nN_i+k-1)\ . \tag{8}$$

The details of its evaluation are discussed in Appendix B. We find

$$\Delta E(q_y)\approx\int dq_x\, U(q_x,q_y)\exp[-q_x^2/2-q_y^2/2]\sqrt{a/2\pi N_s}\ .$$

The energy difference in (8) is proportional to $1/\sqrt{N_s}$ and thus to the momentum differences between site k and site $k-1$, $2\pi/L_y=\sqrt{2\pi a/N_s}$. The net energy change when a particle hops from site q_y to site q_y+p_y is obtained recursively by summing over k. We get in the continuum approximation that

$$E(p_y)\approx[p_y\ln p_y-p_y(1+0.5\ln 8)]/2\pi\ . \tag{8a}$$

This large increase in the diagonal energy is the result of the long-range nature of the Coulomb potential. For short-range potentials, the increase in diagonal energy is linearly proportional to the momentum change; the logarithmic term is absent and the fluctuation then becomes bigger.

The numerical results for E for system sizes $N_s=128$, 512, and 2048 are shown in Fig. 2 for particle (hole) excitations. The excitation is characterized by its distance (y momentum) from the closest clusters; this distance constitutes the x axis in the figures. The energies are all positive, proving that the configuration that we picked is indeed a local minimum. At small distances, the linear dependence is more prominent than the weaker logarithmic correction.

When the interparticle potential U is a δ function, from Eq. (4) $A(j,i)=A(i,j)$. Hence $V=0$. The effective kinetic energy becomes zero; the single-particle states remain degenerate. Hence the case of the δ-function potential seems to be qualitatively different from the Coulomb potential. In that case our calculation is not applicable.

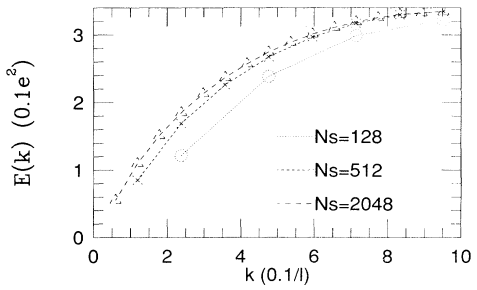

FIG. 2. The self-energy for system sizes $N_s=128$, 512, and 2048 for particle excitations. The excitation is characterized by its distance (y momentum) from the closest clusters; this distance constitutes the x axis in the figures. The energy is measured in units of $e^2/\varepsilon l$.

For particle-hole excitations of total momentum transfer q, the total change in energy is the sum of the particle energy change of momentum q_p and hole energy change of momentum $q-q_p$, $q_p\ln|q_p|+(q-q_p)\ln|q-q_p|$. For small q, this is well approximated by $q\ln|q|$. This can be seen by writing $q_p=xq$ with $0<x<1$. Then the total energy is $q[\ln|q|+x\ln|x|+(1-x)\ln|1-x|]$. For small q, the first term in the square bracket dominates and we obtain the approximation claimed.

B. Renormalization-group calculations

The configuration of the electrons with the lowest diagonal energy can be viewed as an array of 1D chains. The self-energy correction due to the Coulomb potential provides for an effective 1D kinetic energy for the particle-hole excitations away from this configuration. The kinetic energy is now larger by a logarithmic factor than the linear momentum dependence of a 1D electron gas. A 1D electron gas has well-known instabilities that occur at momentum transfer $2k_F=N_c2\pi/L_y$. The 2D density operator ρ is given by

$$\rho(K_y,K_x)=\sum_j \exp(-K^2/2+iK_xj)C^\dagger_{j+K_y/2}C_{j-K_y/2}\ .$$

The 2D density response function $\langle\rho(-K_y,-K_x)\rho(K_y,K_x)\rangle$ is equal to

$$\sum_{q_{1,2}}\exp[-K^2/+iK_x(q_1-q_2)]\times\langle C^\dagger_{q_1+K_y/2}C_{q_1-K_y/2}C^\dagger_{q_2-K_y/2}C_{q_2+K_y/2}\rangle\ .$$

Thus the "$2k_F$ instability" corresponds to a density instability with a periodicity along the y direction.

To treat the intercluster scattering in a more systematic basis, we introduce the cluster momentum q_x and define a basis set

$$|q_x,q_y\rangle=\sum_l \exp(iq_xl)|q_y,l\rangle\ .$$

This kind of basis state has been used in the mean-field CDW calculation[15] and discussed in the small sample calculation.[16] They are eigenstates of two commuting discrete translation operators $\exp i(aC_x)$, $\exp i(2\pi C_y/a)$. $C_{x,y}$ are the center of gyration operators. The labels q_x,q_y are the quantum numbers of the two translation operators and correspond to the x and the y momenta. The ground state we have picked corresponds to the q_y states filled from $-k_F$ to k_F and all possible q_x filled for each of the q_ys. The scattering matrix element can be expressed in this basis.

The usual treatment of the renormalization-group calculation is described in terms of coupling constants $g_{1,2}$ at momentum transfers $2k_F$ and 0. Neglecting the overlap between clusters, we get for momentum transfer $2k_F(g_1)$

$$\langle -k_F,p-q_x;k_F,p'+q_x|H|k_F,p;-k_F,p'\rangle=\sum_x \exp(i2\pi q_x x/N_c)\langle -k_F,l;k_F,l+x|H|k_F,l;-k_F,l+x\rangle$$
$$=\sum_x \exp(i2\pi q_x x/N_c)A[-k_F,k_F(1+2x/\nu),k_F(-1+2x/\nu),k_F]$$
$$=B[-k_F,k_F(1+2x/\nu),k_F(-1+2x/\nu),k_F;q_x]\ . \tag{9}$$

In the notation of Eq. (3), $j_{23}=2k_F$, $j_{13}=2xk_F/\nu$. Performing the sum over x, we obtain $j_x=q_xN_c/2k_F+m\nu N_s/k_F$. Only the $m=0$ term dominates and

$$B[-k_F,k_F(1+2x/\nu),k_F(-1+2x/\nu),k_F;q_x]=U[(j_x^2/a+j_{23}^2a)^{1/2}]\exp[-(j_x^2/a+j_{23}^2a)\pi/N_s]\sqrt{\pi/2N_s}\ .$$

In a similar fashion for small momentum transfer $q_y(g_2)$

$$\langle q_y+k_F,p-q_x;-q_y-k_F,p'+q_x|H|k_F,p;-k_F,p'\rangle$$
$$=\sum_x \exp(i2\pi q_x x/N_c)\langle q_y+k_F,l;-q_y-k_F,l+x|H|k_F,l;-k_F,l+x\rangle$$
$$=\sum_x \exp(i2\pi q_x x/N_c)A[q_y+k_F,-q_y+k_F(-1+2x/\nu),k_F(-1+2x/\nu),k_F]\ .$$

Hence $j_{23}=q_y$, $j_{13}=-q_y+2k_F(1-x/\nu)$. Summing over x, we obtain $j_x=q_xN_c/2k_F+m\nu N_s/k_F$. The matrix element thus becomes

$$U[(q_x^2+q_y^2)^{1/2}]\exp[-\pi\nu(q_x/2k_F)^2/a-a_y^2/2]$$
$$\times\cos[2\pi q_x(2k_F-q_y)/N_s]\sqrt{\pi/2N_s}\ .$$

The g's defined in the 1D problem are related to the coefficients B defined above by $g=L_yB$. Since $B\approx N_s^{0.5}$, g remains constant as the system size is increased.

As we see from the above, for the present 2D problem, these matrix elements also depend on the additional x momentum. We capture this effect with an additional subscript by focusing on coupling constants g_{ij} with $j=1(2)$ corresponding to large (small) x momentum and $i=1(2)$ corresponding to large (small) y momentum.

The infrared divergence is not expected to affect the response function at small momentum transfers. A zeroth-order approximation that deals with the long-range nature of the Coulomb potential is the random-phase approximation (RPA), from which we get $\chi=\chi_0/[1+\nu(q)\chi_0]$. Displaying the real and imaginary part explicitly we obtain $\chi^{-1}\approx\nu(q)-i\omega/q^2\sigma$. Thus the detail nature of χ_0 is overwhelmed by the Coulomb interaction. In the same vein the small momentum transfer interaction g_{22}, being proportional to $1/q$, is divergent and needs to be screened. In the RPA we get $g(p)=g^0(p)/[1+g^0(p)\chi_0]$, where g^0 is the unscreened coupling constant. To obtain more quantitatively reliable results, the screening should be more carefully treated. In this paper, we shall focus more on elucidating the physics and shall settle for the RPA for the screening. The contribution from the skeleton bubble χ_0 is nonzero only if the particle and the hole came from the same cluster. It can be easily evaluated and is found to be $\chi_0=1/\ln(q)$. Thus $g_{22}\approx h_2\ln(q)$ where h_2 is nondivergent as $q\to 0$.

For short-range interactions, all the screening is not necessary while the energy denominator remains linearly proportional to the momentum change. Both the zero momentum channel and the $2k_F$ momentum channel are logarithmically divergent.

We shall assume that the magnetic field is high enough that all spins are aligned. In our problem g_2 is much larger than g_1 because the latter involves a much smaller overlap. An estimate of the initial value of the $2k_F$ matrix element can be obtained from the Hamiltonian. Within the same chain $g_1=0.38$, and between the nearest-neighbor chains $g_1(\Delta l=1)=0.000\,595$. These can be Fourier transformed to obtain the coefficients $g_1(p)$. Because $g_1(\Delta l)$ dies off rapidly as a function of the cluster separation Δl, its Fourier transform $g_1(p)$ is not a strong function of p. Hence $g_{12}^0\approx g_{11}^0$. As we shall see, because of the weak interchain backward scattering coupling constant g_1, the 2D CDW fixed point is never reached for practical purposes.

The parquet diagrams for coupled 1D chains have been discussed by Gor'kov and Dzyaloshinskii[17] and the RG equations have been discussed by Lee, Rice, and Klemm.[18] For a 1D electron gas, because of the cancellation between the Cooper and the zero-sound channel, a CDW instability does not develop for a repulsive (positive) g_1. For coupled chains $g_1(p)$ first scales toward zero. Because of interchain coupling, the backward scattering matrix element exhibits a momentum dependence. Because of this eventually at certain momentum p_c, $g_1(p_c)$ becomes negative and eventually an infinitely sharp peak is developed such that $g_1(p_c)\to-\infty$. It is not difficult to modify their result for the present problem.

The diagrams for the vertex function to the lowest order are essentially identical to those in the 1D calculation[18] and are shown in Fig. 3. The lines in the Feynman diagrams of Fig. 3 are propagators with the Hartree-Fock self-energy corrections incorporated. We keep track of the momentum dependence of the matrix elements with the notation $g(j23,j13,p)$. The scattering amplitudes corresponding to Figs. 3(a)–3(h), are, respectively,

$$\int dq_3 dp' g(2k_F+q_3,q_3,p')g(2k_F+q_3,q_3,p-p')\theta(q_3>0)/[2\pi v q_3 \ln(q_3)] ,$$
$$\int dq_3 dp' g(2k_F+q_3,q_3,p')g(q_3,q_3+2k_F,p-p')\theta(q_3>0)/[2\pi v q_3 \ln(q_3)] ,$$
$$\int dq_3 dp' g(q_3,2k_F+q_3,p')g(q_3,2k_F+q_3,p-p')\theta(q_3>0)/[2\pi v q_3 \ln(q_3)] ,$$
$$\int dq_3 g(2k_F,q_3,p)^2\theta(q_3>0)/[2\pi v q_3 \ln(q_3)] , \quad (10)$$
$$\int dq_3 dp' g(2k_F,q_3,p)g(q_3,q_3+2k_F,p')\theta(q_3>0)/[2\pi v q_3 \ln(q_3)] ,$$
$$\int dq_3 dp' g(q_3,2k_F,p')g(q_3,2k_F,p-p')\theta(q_3>0)/[2\pi v q_3 \ln(q_3)] .$$

In the conventional 1D RG calculation, there is a cancellation of the scattering amplitudes between the Cooper and the zero-sound channel. In the present case because of the momentum dependence of the matrix elements the cancellation between these two types of terms becomes incomplete. However, the incomplete cancellation only provides for nonlogarithmic correction in the second-order diagram here.

Recall that $g_{22} \propto \ln q$, for scattering amplitudes involving g_{22}, this logarithmic factor is canceled out by the additional logarithmic factor in the energy denominator and one ends with the same logarithmic amplitudes as in the conventional 1D problem. The large momentum (x or y) transfer scattering matrix elements g_{1i}, g_{21} are not divergent and are not strongly affected by screening. Thus scattering involving these is more suppressed by the energy cost, the corresponding scattering amplitude is proportional to $\ln[\ln(q_c)]$ rather than $\ln(q_c)$ (q_c is the cutoff) as in the conventional 1D problem.

We obtain the first-order RG equations:

$$g'_{11}(p) = -[g_{11}^2 + g_{21}(g_{11}-g_{12})]/2\pi v x , \quad (11a)$$
$$g'_{12}(p) = -[g_{12}^2 - g_{21}(g_{11}-g_{12})]/2\pi v x , \quad (11b)$$
$$g'_{21} = -g_{11}g_{12}/\pi v x , \quad (11c)$$

where the prime denotes differentiation with respect to $x = \ln[\min(q,\omega)]/E_F$. As ω approaches zero, x approaches $-\infty$. The lowest-order perturbation series for the small momentum transfer scattering is given by

$$g_{22} = h_2 x + (g_{11}^2 + g_{12}^2)\ln|x| .$$

The divergence due to higher-order scattering is weaker than the bare divergence due to the long-range nature of the potential. In addition g_{1j} is small, thus it is a good approximation to assume that g_{22} remains unchanged.

We have solved Eq. (11) numerically with a sixth-order Runge-Kutta algorithm in double precision. The scaling trajectories are shown in Fig. 4. We find that the coupling constants remain basically unchanged. This is consistent with the fixed point at $g_{11}=g_{12}=g_{11}^0/(1+g_{11}^0 \ln|x|/2\pi v)$. A stability analysis about this fixed point shows that the difference $\delta g = g_{11}-g_{12}$ changes according to the equation

$$(\delta g)' = 2(g_{21}^0 - g_{11}^0)\delta g/2\pi v x .$$

Thus

$$\delta g = \delta g^0 (x/x^0)^{2(g_{21}^0 - g_{11}^0)/2\pi v} .$$

The difference can increase in principle. However, for practical purposes the initial difference is small enough and the power small enough that this does not seem to happen over large length scales. This is consistent with the result of Chui, Ma, and Hakim[7] who studied a series of variational wave functions with different amounts of

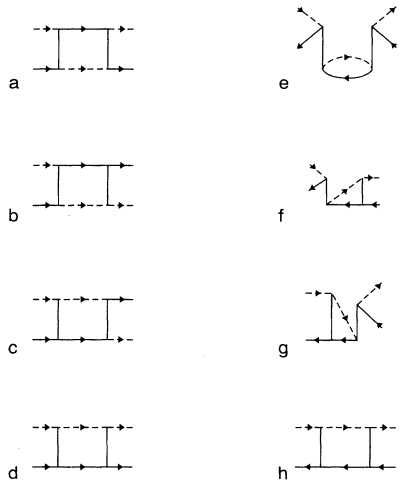

FIG. 3. Second-order vertex diagrams for the Cooper channels (a)–(d) and the zero-sound channels (e)–(h). An electron near $+k_F$ ($-k_F$) is denoted by a solid (dashed) line.

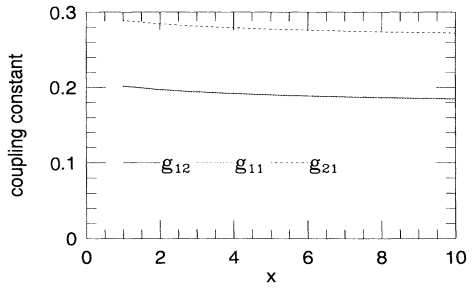

FIG. 4. The scaling trajectory of some typical g's as a function of the scaling variable x.

fluctuations and found that the wave function with the largest fluctuation is the lowest in energy. They found that the highly fluctuating wave function is stabilized by the exchange energy. Structure factors computed from exact diagonalization of small clusters of 4, 8, and 16 particles increase as the system size is increased,[8] also consistent with this interpretation. In the present diagrammatic language, it is the exchange diagrams that cancel out the CDW instability and generate the large fluctuations.

For the half-filled case, there are additional diagrams that come from scattering from one cluster to the next. These correspond to the umklapp scattering in the half-filled Hubbard model. These diagrams provide also for corrections that are also of the order of $\{\ln[\ln(q)]\}^n$ and thus are not expected to change the coupling constants much.

IV. CONCLUSION

In this paper a first-order renormalization-group calculation is carried out for the coupling constants characterizing the two-particle vertex function. We find that the coupling constants remain unchanged as the system size is increased, consistent with the interpretation of a marginal solid.

One obvious experimental test for the present picture would be a divergent structure factor. Because the coupling coefficient remains fairly constant, the single-particle excitation energy will remain close to its bare value in Eq. (8a), $p \ln p$. This is similar to the single-particle energy found by Halperin, Lee, and Reed[11] starting from the fluid. Thus the small momentum transfer response functions such as the conductivity will be similar in the two cases. In particular, in the small frequency limit in the random-phase approximation, the inverse response function is given by $v(q)-i\omega/q^2\sigma$; the bare response function is overwhelmed by the Coulomb potential $v(q)$. This is the same in both their state and ours. Thus this function, which may be related to the surface-acoustic-wave measurement, would not be a sensitive enough test to distinguish between the two scenarios. Measurements such as the magnetoresistance oscillation that Halperin, Lee, and Reed suggested may distinguish between the two pictures. We iterate our point made in the Introduction, that if the mass at the Fermi surface found by Halperin, Lee, and Reed is infinite, the total energy can be lowered by arranging the system in a periodic structure at little cost to the kinetic energy. Thus the fluid phase they discuss should be unstable towards some kind of charge-density-wave formation.

In this paper we have employed the Landau gauge. Our results are not really gauge dependent. As we have discussed,[3] one can employ the circular gauge and a similar discussion can be carried out. For example, the unperturbed ground state will be clusters of states with contiguous angular momenta m instead of clusters of contiguous y momenta j.

The calculation presented here does not work at low densities. We have calculated the effective self-energy for a lower density at $\nu=\frac{1}{7}$. The result for $N_s=1792$ is shown in Fig. 5. The energy is shown up to be a distance

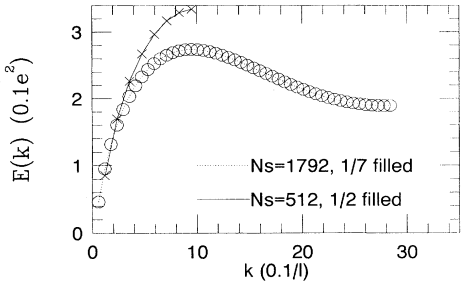

FIG. 5. The effective self-energy for filling factors $\nu=\frac{1}{7}$, $N_s=1792$ and $\nu=\frac{1}{3}$, $N_s=768$. The maximum distance is half the length of the empty space between the clusters.

of half the empty space between the clusters. For comparison, we have reproduced the results at $\frac{1}{2}$ filled in the same diagram. Whereas at short distances the energy dependence is very close for the two filling factors, at large distances they are very different. For the lower density case an additional minimum in the particular-hole excitation spectrum is developed at half the distance in between the clusters. This suggests that a perturbation expansion from the cluster configurations is not appropriate at very low densities and is consistent with our expectation that a solid phase with true long-range positional order will form at very low densities.

APPENDIX A

In this paper we pick our "ground state" $|G\rangle$ to be composed of clusters of N_c contiguous sites occupied with each cluster surrounded by $N_c(1/\nu-1)/2$ empty sites on both its left- and right-hand side. These units are then joined together to form the total system. For example, at $\frac{1}{3}$ filled, the particles tend to form clusters of approximately 2 for the 12-site case and clusters of 4 in the 48-site case. This is approximately seen in the small sample diagonalizations of the Hamiltonian. This we discuss below.

For $N_s=12$ and as aspect ratio of 1.1547, the ground state, which include all fluctuations, is dominated by configurations of 1 cluster of 2 and 2 clusters of 1 with a probability density of 0.473 $[0.344(|1,4,8,9\rangle+|1,5,6,10\rangle+|2,3,7,10\rangle-|4,7,11,12\rangle)]$, of clusters of 2 with a probability density 0.306 $[0.391(|5,6,11,12\rangle-|2,3,8,9\rangle)]$, of 4 clusters of 1 equally spaced at distance 2 apart with a probability density 0.149 $[-0.386|1,4,7,10\rangle]$, and 4 clusters of 1 but spaced at distances 3,3,1,1 with a probability density 0.047 $[-0.108(|1,5,7,9\rangle+|2,4,6,10\rangle-|4,8,10,12\rangle-|1,3,7,11\rangle)]$. The total sum of these probability densities adds up to 0.975. For an aspect ratio of 1, the effective cluster size is reduced. The ground state is dominated by configurations of 1 cluster of 2 and 2 clusters of 1 with a probability density of 0.568 $[0.377(|1,4,8,9\rangle+|1,5,6,10\rangle+|2,3,7,10\rangle-|4,7,11,12\rangle)]$, of 2 clusters of 2 with a probability density of 0.191 $[0.3088(|5,6,11,12\rangle-|2,3,8,9\rangle)]$, of 4 clusters of 1 equally spaced at distance 2 apart with a proba-

bility density 0.09 $[-0.302|1,4,7,10\rangle]$, and 4 clusters of 1 but spaced at distances 3,3,1,1 with a probability density 0.13 $[-0.182(|1,5,7,9\rangle+|2,4,6,10\rangle-|4,8,10,12\rangle-|1,37,11\rangle)]$. The total sum of these probability densities adds up to 0.979. The probability density for the configuration with 2 clusters of 2 is reduced in magnitude.

APPENDIX B

In this appendix we derive the effective kinetic energy for particle excitations. This can be done by substituting Eqs. (7) and (3) into Eq. (8). As we see from Eq. (7) there is a direct contribution E_d with $j_{23}=0$ and an exchange contribution E_e with $j_{13}=0$.

$$\Delta E(k)=E_d-E_e \ .$$

For the direct contribution, performing the sum over n, we obtain $j_x=mN_c$ for integer m. Since j_{23} and j_x cannot both be zero (neutral background), the $m=0$ term is not allowed. We obtain

$$E_d=4N_c\sum_{m=1}^{\infty}U[mN_c/a^{1/2}]\exp[-(mN_c)^2\pi/aN_s]\{\cos[2\pi mN_c(N_c+k-1)/N_s]-\cos[2\pi mN_c(k-1)/N_s]\}\sqrt{\pi/2N_s} \ .$$

There is a factor of 2 from contributions with $m<0$. The other factor of 2 comes from Eq. (7). Because of the exponential factor, this is dominated by the $m=1$ term and

$$\begin{aligned}E_d&\approx 4N_cU[N_c/a^{1/2}]\exp[-0.5\pi/a]\{-2\cos[\pi(k-1)/N_c]\}\sqrt{\pi/2N_s}\\&\approx 4a^{1/2}\exp[-0.5\pi/1]\cos[\pi(k-1)/N_c]/\sqrt{1/2N_s\pi} \ .\end{aligned}$$

The exchange contribution comes from terms with $j_{13}=0$.

$$\begin{aligned}E_e=2\sum_{n=0}^{n=N_c-1}\sum_{j_x=-\infty}^{\infty}&(U\{[j_x^2/a+(nN_i+N_c+k-1)^2a]^{1/2}\}\exp\{-[j_x^2/a+(nN_i+N_c+k-1)^2a]\pi/N_s\}\\&-U\{[j_x^2/a+(nN_i+k-1)^2a]^{1/2}\}\exp\{-[j_x^2/a+(nN_i+k-1)^2a]\pi/N_s\})\sqrt{\pi/2N_s} \ .\end{aligned}$$

In the exchange contribution, because of the exponential cutoff, only the term with $n=0$ needs to be kept. We thus get

$$\begin{aligned}E_e=2\sum_{j_x=-\infty}^{\infty}&(U\{[j_x^2/a+(N_c+k)^2a]^{1/2}\}\exp\{-[j_x^2/a+(N_c+k)^2a]\pi/N_s\}\\&-U\{[j_x^2/a+(k-1)^2a]^{1/2}\}\exp\{-[j_x^2/a+(k-1)^2a]\pi/N_s\})\sqrt{\pi/2N_s} \ .\end{aligned}$$

The dominant contribution comes from the second term. In the continuum limit, it is approximately equal to[19]

$$\begin{aligned}\Delta E(q_y)&\approx\int dq_x(q_x^2+q_y^2)^{-0.5}\\&\quad\times\exp[-q_x^2/2-q_y^2/2]\sqrt{a/2\pi N_s}\\&\approx 0.5\exp(q_y^2/4)K_0(q_y^2/4)\sqrt{a/2\pi N_s} \ .\end{aligned}$$

The net energy change when a particle hops from site q_y to site q_y+p_y is obtained recursively by summing over k. We get in the continuum approximation that

$$\begin{aligned}E(p_y)&\approx 0.5\int dq_y\ln(q_y^2/8)/2\pi\\&\approx[p_y\ln p_y-p_y(1+0.5\ln 8)]/2\pi \ .\end{aligned}$$

[1] R. Willett, J. P. Eisenstein, H. L. Stormer, D. C. Tsui, A. C. Gossard, and J. H. English, Phys. Rev. Lett. **59**, 1776 (1987).
[2] S. T. Chui, Phys. Rev. Lett. **56**, 2395 (1986).
[3] S. T. Chi, Phys. Rev. B **36**, 2806 (1987).
[4] G. Timp *et al.*, Phys. Rev. Lett. **63**, 2268 (1989).
[5] H. W. Jiang, H. L. Stormer, D. C. Tsui, L. N. Pfeiffer, and K. W. West, Phys. Rev. B **40**, 12 013 (1989).
[6] S. T. Chui, Phys. Rev. B **42**, 5339 (1990).
[7] S. T. Chui, K. B. Ma, and T. Hakim, Phys. Rev. B **33**, 7110 (1986).
[8] S. T. Chui and Timothy Ziman, J. Phys. Condens. Matter **5**, L269 (1993).
[9] Y. Kuramoto and R. R. Gerhardts, J. Phys. Soc. Jpn. **51**, 3810 (1982).
[10] G. Fano, F. Ortolani, and E. Tosatti, Il Nuovo Cimento D **9**, 1337 (1987).
[11] B. I. Halperin, P. A. Lee, and N. Reed, Phys. Rev. B **47**, 7312 (1993).
[12] R. Willett *et al.* (unpublished).
[13] H. Stormer *et al.* (unpublished).
[14] S. T. Chui, Phys. Rev. B **32**, 8438 (1985).
[15] D. Yoshioka and P. A. Lee, Phys. Rev. B **27**, 4986 (1983).
[16] D. Haldane, Phys. Rev. Lett. **55**, 2095 (1985).
[17] L. P. Gorkov and I. E. Dzyaloshinskii, Zh. Eksp. Teor. Fiz. **67**, 397 (1974) [Sov. Phys. JETP **40**, 198 (1975)].
[18] P. A. Lee, T. M. Rice, and R. A. Klemm, Phys. Rev. B **15**, 2984 (1977).
[19] A. P. Prudnikov, Yu. A. Brychkov, and O. I. Marichev, *Integrals and Series* (Gordon and Breach, New York, 1986), p. 324, Eq. 2.3.6(10).